

Cite this: DOI: 10.1039/c4nj00735b

Saturated deep-blue emitter based on a spiro[benzoanthracene–fluorene]-linked phenanthrene derivative for non-doped organic light-emitting diodes

Houjie Liang,^{ab} Xinxin Wang,^c Xingye Zhang,^a Zhiyang Liu,^a Ziyi Ge,^{*a} Xinhua Ouyang^{*a} and Suidong Wang^{*c}

A spiro[benzoanthracene–fluorene] derivative containing a phenanthrene moiety, 2',3-di(phenanthren-9-yl)spiro[benzo[de]anthracene-7,9'-fluorene] (**DPSBAF**), was prepared by a Suzuki coupling reaction. The photophysical and photochemical properties were investigated systematically. A non-doped organic light-emitting diode using **DPSBAF** as the emitter achieved a luminance efficiency of 2.18 cd A⁻¹ with Commission Internationale de l'Éclairage 1931 chromaticity coordinates of (0.15, 0.09). The synthesized spiro[benzoanthracene–fluorene] derivative with a high thermal stability, a glass transition temperature of 210 °C and a decomposition temperature of 410 °C, shows potential for application in non-doped saturated deep-blue organic light-emitting diodes.

Received (in Montpellier, France)
6th May 2014,

Accepted 20th June 2014

DOI: 10.1039/c4nj00735b

www.rsc.org/njc

1. Introduction

Organic light-emitting diodes (OLEDs) have attracted sustained attention for their potential applications in both full-color displays and solid-state lighting.^{1–5} Although OLEDs have recently been employed in small display panels, their wider application in the mainstream display panel market will depend on the development of blue electroluminescent (EL) materials.^{6–8} Compared with green and red OLEDs, it is difficult to obtain non-doped deep-blue electroluminescent materials with a Commission Internationale de l'Éclairage (CIE) coordinate of $y < 0.15$ due to the intrinsic wide band gap nature of deep-blue emitters.^{8–10} Fisher *et al.* reported luminance efficiencies (LEs) of 0.47 cd A⁻¹ and 1.49 cd A⁻¹ for a spin-coated device and an evaporated device with CIE coordinates of (0.156, 0.069) and (0.157, 0.079).¹¹ Linton *et al.* showed external quantum efficiencies (EQEs) of 0.20% and 0.54% for oxadiazole derivatives applied as deep-blue emitters with CIE coordinates of (0.158, 0.120) and (0.164, 0.114), respectively.⁵ 3,7-Bis(9,9-bis(6-(9H-carbazol-9-yl)hexyl)-9H-fluoren-2-yl)dibenzo[*b,d*]-thiophene 5,5-dioxide (TCSoc) was reported by Yao *et al.* as a blue emitter in solution-processed OLEDs, which achieved a LE of 1.6 cd A⁻¹, but insufficient deep-blue CIE

coordinates were shown (0.16, 0.16).¹² Recently, Ma *et al.* reported 3,7-bis(9,9,9',9'-tetrakis(6-(9H-carbazol-9-yl)hexyl)-9H,9'H-[2,2'-bifluoren]-7yl)dibenzo[*b,d*]thiophene showing a deep-blue emission with CIE coordinates of (0.17, 0.09) and a LE of 0.9 cd A⁻¹.¹³ Although many deep-blue fluorescent materials have been developed in the past decade, saturated deep-blue emitters with a CIE coordinate of $y < 0.10$ should be further investigated.^{10,14–17}

Spiro compounds have evolved as promising optoelectronic materials with high glass transition temperatures (T_g) and solubility.^{18,19} Asymmetrical spiro[benzoanthracene–fluorene] derivatives possessing a naphthalene group are one kind of spiro compound which have recently been used in OLEDs.²⁰ Gong *et al.* introduced spiro[benzoanthracene–fluorene]/carbazole compounds as host materials for orange phosphorescent OLEDs with twisted structures in 2012.²⁰ Subsequently, Kim *et al.* reported a series of novel spiro[benzoanthracene–fluorene] derivatives as host materials and obtained sky-blue fluorescent emissions.²¹ Recently, we demonstrated that spiro[benzoanthracene–fluorene]/benzimidazole could be used as a non-doped deep-blue emitter with CIE coordinates of (0.15, 0.10).²² Relatively little attention has been paid to non-doped saturated deep-blue OLEDs with spiro[benzoanthracene–fluorene] derivatives as emitters. Therefore, it is desirable to develop non-doped saturated deep-blue OLEDs based on spiro[benzoanthracene–fluorene] derivatives.

In this work, we designed and synthesized 2',3-di(phenanthren-9-yl)spiro[benzo[*de*]anthracene-7,9'-fluorene] (**DPSBAF**) due to the high thermal stability of the spiro[benzoanthracene–fluorene] moiety and the low conjugation of the phenanthrene unit,

^a Ningbo Institute of Materials Technology & Engineering, Chinese Academy of Sciences, Ningbo 315201, China. E-mail: geziyi@nimte.ac.cn, ouyangxh@nimte.ac.cn

^b University of Chinese Academy of Sciences, Beijing 100049, China

^c Institute of Functional Nano & Soft Materials, Soochow University, Suzhou 215123, China. E-mail: wangsd@suda.edu.cn

which can improve the color purity.^{9,20} The twisted and rigid structure of **DPSBAF** prevents close-packing and effectively inhibits fluorescence quenching in the film.^{23–27} The non-doped saturated deep-blue OLED employing **DPSBAF** as the emitter achieved a maximum luminance efficiency of 2.18 cd A⁻¹ with CIE coordinates of (0.15, 0.09), which is very close to the National Television System Committee (NTSC) blue standard.

2. Experimental

2.1. Measurements and characterization

Nuclear magnetic resonance (NMR) spectra were recorded on a Bruker DRX-400 spectrometer. High-resolution mass spectra (HRMS) were recorded on a Bruker Esquire LC/Ion Trap Mass Spectrometer and JEOL/HX-110. Elemental analyses were obtained with a Perkin-Elmer 2400 II elemental analyzer. Differential scanning calorimetry (DSC) curves were measured using a Mettler Toledo DSC 822 instrument with a heating rate of 20 °C min⁻¹ under nitrogen flushing. Thermogravimetric analyses (TGAs) were carried out using a Perkin-Elmer Pyris thermogravimeter under nitrogen gas at a heating rate of 10 °C min⁻¹. UV-vis absorption spectra were recorded on a Perkin-Elmer Lambda 950 spectrophotometer. Fluorescence (PL) measurements were carried out with a FLSP 920 spectrophotometer in a 10⁻⁶ mol L⁻¹ solution and in the solid state. The electrochemical properties of **DPSBAF** were studied through cyclic voltammetry (CV) on a CHI 660D electrochemical workstation with a Pt disk as the working electrode, a Pt wire as the counter electrode, and Ag/AgCl as the reference electrode, in a dichloromethane solution containing 0.1 M of tetrabutylammonium hexafluorophosphate as the supporting electrolyte.

2.2. Synthesis of the compounds

The compounds 1,8-diiodonaphthalene (**1**),²⁸ 1-iodo-8-phenylnaphthalene (**2**),²⁹ 2'-bromospiro[benzo[*de*]anthracene-7,9'-fluorene] (**2'-Br-SBAF**)²⁰ and 2',3-dibromospiro[benzo[*de*]anthracene-7,9'-fluorene] (**2',3-dBr-SBAF**)²² were synthesized according to or slightly modified literature procedures.

2',3-Di(phenanthren-9-yl)spiro[benzo[*de*]anthracene-7,9'-fluorene] (DPSBAF). **2',3-dBr-SBAF** (1.0 g, 2.0 mmol), phenanthren-9-ylboronic acid (1.0 g, 4.6 mmol), Pd(PPh₃)₂Cl₂ (0.20 g, 0.28 mmol) and toluene (150 mL) were stirred in a three-necked flask for 30 min. Potassium carbonate (2 M, 20 mL) and anhydrous ethanol (30 mL) were added to the above solution. The resulting solution was refluxed for 3 days at 105 °C. The reaction mixture was extracted with dichloromethane. After the organic layer was evaporated using a rotary evaporator, the resulting powdery product was purified by column chromatography to give a white solid. Yield 93.9%. ¹H NMR (400 MHz, CDCl₃) δ 8.85–8.79 (m, 2H), 8.75–8.86 (m, 2H), 8.37 (t, 1H, *J* = 7.28 Hz), 8.30 (d, 1H, *J* = 7.99 Hz), 8.04–7.53 (m, 16H), 7.50–7.29 (m, 6H), 7.25–7.06 (m, 4H), 6.85–6.77 (m, 2H). ¹³C NMR (400 MHz, CDCl₃) δ 157.30, 157.15, 156.85, 140.94, 140.85, 139.99, 139.66, 139.16, 138.86, 138.60, 138.53, 137.48, 137.30, 133.46, 132.16, 131.91, 131.69, 131.48, 130.99, 130.66, 130.41, 130.31, 129.91, 129.78, 129.66, 128.74, 128.60, 128.33, 127.81, 127.68, 127.60, 127.44, 127.38, 127.20, 126.93, 126.78, 126.69, 126.57,

126.41, 125.84, 125.57, 125.43, 125.31, 125.24, 123.48, 122.86, 122.68, 122.51, 120.33, 120.25, 120.03, 119.18, 60.04. HRMS (*m/z*): calcd for (M⁺) C₅₇H₃₄ 718.2661; found 718.4522. Anal. calcd for C₅₇H₃₄: C 95.23, H 4.77; found: C 95.14, H 4.80.

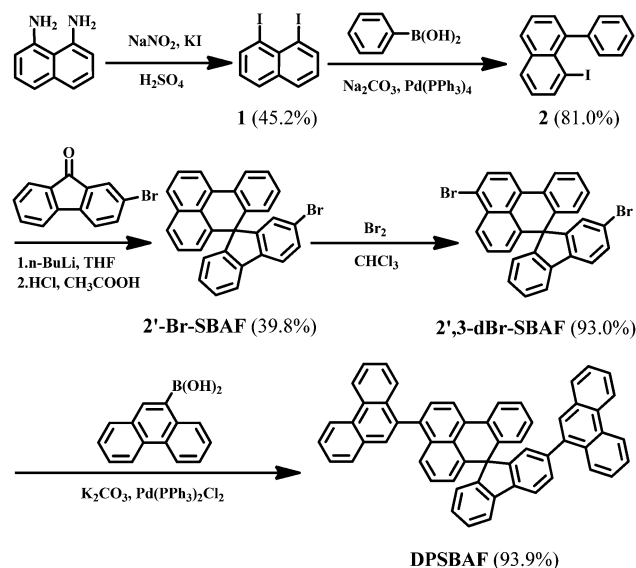
2.3. Device fabrication and characterization

DPSBAF was purified twice by vacuum sublimation with the tube heating up to 340 °C. The compound was deposited for 6 h at 5 × 10⁻⁴ Pa before the OLED fabrication. The device configuration of ITO/MoO₃ (5 nm)/NPB (40 nm)/TCTA (5 nm)/**DPSBAF** (30 nm)/B3PyPB (40 nm)/LiF (1 nm)/Al (100 nm) was fabricated by vacuum deposition. All of the organic layers and inorganic layers were prepared in sequence at 10⁻⁶ Torr. The electroluminescence spectra and the Commission Internationale de l'Éclairage coordination of the device were measured using a PR655 spectra scan spectrometer. The luminance–current and density–voltage characteristics were recorded simultaneously from the measurement of the EL spectra by combining the spectrometer with a Keithley 2400 programmable voltage–current source. All measurements were carried out at room temperature under ambient conditions.

3. Results and discussion

3.1. Synthesis

The synthetic route and structure of **DPSBAF** are shown in Scheme 1. Compound **1** was synthesized *via* the Sandmeyer reaction of 1,8-diaminonaphthalene. A Suzuki coupling reaction of compound **1** with phenylboronic acid yielded compound **2**. Compound **2** was treated with *n*-BuLi and 2-bromo-9*H*-fluoren-9-one at –78 °C to give an aromatic alcohol intermediate. Then compound **2'-Br-SBAF** was obtained through a Friedel–Crafts reaction with HCl and acetic acid as catalysts. A bromination reaction was employed in the synthesis of **2',3-dBr-SBAF** with a yield of over 90%. **DPSBAF** was obtained by a Suzuki coupling



Scheme 1 The synthetic route to **DPSBAF**.

Table 1 Thermal properties, photophysical properties and electrochemical properties of blue emitters

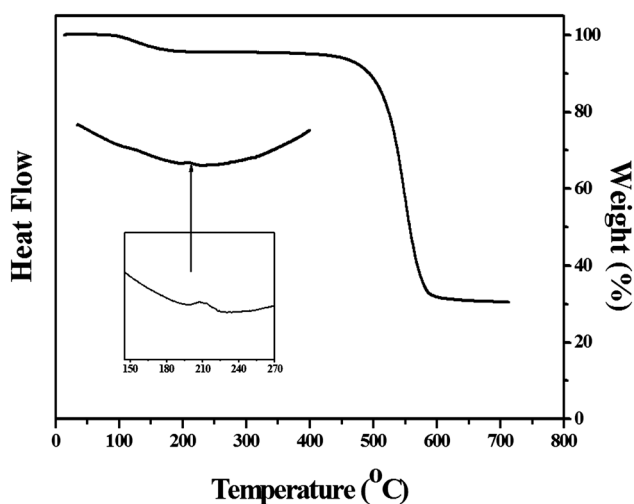
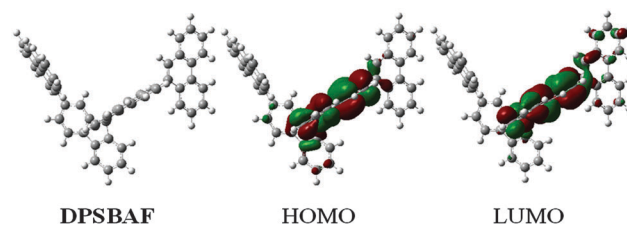
	Compound		
	DPSBAF	DPSF (ref. 9)	SAFBI (ref. 22)
T_g (°C)	210	178	—
T_d (°C)	410	503	426
λ_{\max} Abs ^a (nm)	320	254	325
λ_{\max} PL ^a (nm)	418	383	440
λ_{\max} PL ^b (nm)	422, 425	398	456
HOMO ^c (eV)	-5.77	-5.8	-5.62
LUMO ^d (eV)	-2.48	-2.3	-2.51

^a Measured in CH₂Cl₂, ^b Measured as a solid film on quartz plates. ^c Highest occupied molecular orbital by cyclic voltammetry. ^d Estimated based on absorption onset and HOMO.

reaction in aqueous potassium carbonate solution. Further details are given in the Experimental section. **DPSBAF** was characterized by ¹H NMR spectroscopy, ¹³C NMR spectroscopy, HRMS and elemental analysis. **DPSBAF** was found to be soluble in many common organic solvents such as dichloromethane, chloroform, THF and toluene.

3.2. Thermal properties

The thermal properties of **DPSBAF** were measured by differential scanning calorimetry and thermogravimetric analysis under a nitrogen atmosphere, and the data is shown in Table 1 and Fig. 1. The glass transition temperature of **DPSBAF** was found to be 210 °C and no obvious melting transition (T_m) was observed even when heated up to 400 °C. This result indicates that the highly twisted structure might mitigate the intermolecular interactions of **DPSBAF** in the solid state.²³ From the TGA result, **DPSBAF** exhibited a decomposition temperature (T_d , corresponding to 5% weight loss) as high as 410 °C. Such a high T_d value indicates that **DPSBAF** is stable and has the potential to be used as an emitter by vacuum thermal evaporation.^{30–32}

**Fig. 1** DSC trace of **DPSBAF** recorded at a heating rate of 20 °C min⁻¹ and TGA thermogram of **DPSBAF** recorded at a heating rate of 10 °C min⁻¹.**Fig. 2** The optimized geometry and molecular orbital distribution of **DPSBAF**.

3.3. Theoretical calculations

The ground-state geometry of **DPSBAF** in a vacuum was optimized by density functional theory (DFT) with the B3LYP functional and the basis set 6-31G(d,p) using the Gaussian 03 program. The frontier molecular orbitals were drawn using an isovalue of 0.02 a.u. As shown in Fig. 2, the HOMO and LUMO of **DPSBAF** were located at the **SBAF** core. The twisted geometry of **DPSBAF** could efficiently prevent recrystallization in the film due to the large torsional stresses, which can induce the formation of either an exciplex or excimer.⁸ The HOMO and LUMO energy levels of **DPSBAF** were calculated to be -5.35 eV and -1.39 eV, respectively.

3.4. Optical properties

The UV-vis absorption and PL spectra of **DPSBAF** in diluted CH₂Cl₂ solution and as a solid film spin-coated on quartz plates were explored as shown in Fig. 3. The photophysical data of the compound are summarized in Table 1. **DPSBAF** showed a UV-vis absorption maximum at 320 nm, which is attributed to the π - π^* transition of the spiro[benzoanthracene-fluorene] core in the CH₂Cl₂ solution.²⁰ Compared with the absorbance in solution, the main absorption peak in the film was blue-shifted and the long wavelength absorption was much weaker. These differences could be explained by the formation of H-aggregation.^{33–35} Furthermore, **DPSBAF** exhibits a fluorescence peak at 418 nm in dilute CH₂Cl₂ solution. In the film state, **DPSBAF** shows dual emission peaking at 422 nm and 425 nm. The emission λ_{\max} in the film was slightly red-shifted compared with the diluted solution, which can be attributed

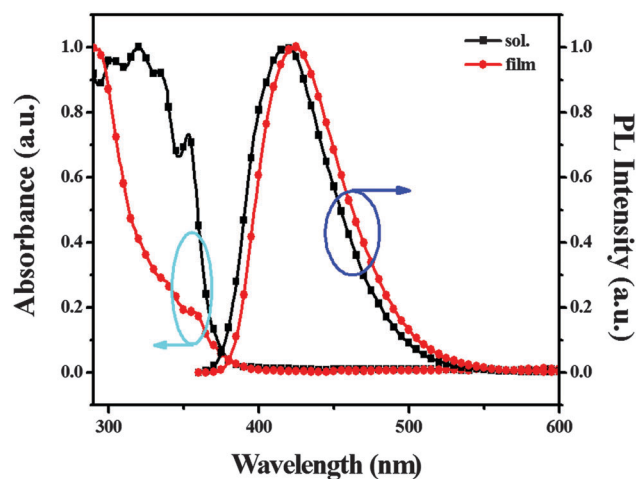
**Fig. 3** UV absorption and PL spectra of **DPSBAF** in CH₂Cl₂ and in the film state.

Table 2 Electroluminescent characteristics of OLEDs

	Compound		
	DPSBAF	DPSF (ref. 9)	SAFBI (ref. 22)
V_{on}^a (V)	3.7	4.5	—
λ_{max} EL (nm)	448	—	436
LE_{max} (cd A^{-1})	2.18	1.97	1.96
PE^c (lm W^{-1})	1.59	—	—
EQE_{max} (%)	2.87	3.41	2.23
CIE^c (x, y)	(0.15, 0.09)	(0.15, 0.08)	(0.15, 0.10)

^a Turn-on voltage at 1 cd m^{-2} . ^b Values collected at 1 mA cm^{-2} . ^c Values collected at 20 mA cm^{-2} .

to the twisted structure of DPSBAF preventing close molecular packing in the solid film.²³

3.5. Electrochemical properties

Cyclic voltammetry analysis was carried out to study the HOMO energy level of DPSBAF, and the result is shown in Table 2 and Fig. 4. The HOMO value was calculated from $\text{HOMO} = -([E_{\text{onset}}]_{\text{ox}} + 4.4)$.³⁶ The onset oxidation potential of DPSBAF was 1.37 V during the anodic scan in CH_2Cl_2 and the HOMO value of DPSBAF was -5.77 eV . The energy band gap of DPSBAF, which was estimated by analysing the absorption edge of the UV-vis curve, was 3.29 eV . The LUMO level of DPSBAF, calculated from $\text{HOMO} + E_g^{\text{opt}}$, was -2.48 eV .

3.6. Electroluminescent properties

The non-doped OLED device was fabricated with a structure of ITO/MoO₃ (5 nm)/NPB (40 nm)/TCTA (5 nm)/DPSBAF (30 nm)/B3PyPB (40 nm)/LiF (1 nm)/Al (100 nm). Indium tin oxide (ITO) and Al were utilized as the anode and cathode, MoO₃ was used as a hole injecting layer, *N,N'*-bis(naphthalene-1-yl)-*N,N'*-bis(phenyl)-benzidine (NPB) was used as a hole transporting layer, 4,4',4''-tri(*N*-carbazolyl)benzene (TCTA) was used as an electron blocking layer, 3,3'',5,5''-tetra(pyridin-3-yl)-1,1':3',1''-terphenyl (B3PyPB)^{37,38} was used as an electron transporting and hole blocking layer, and LiF was used as an electron injecting layer.

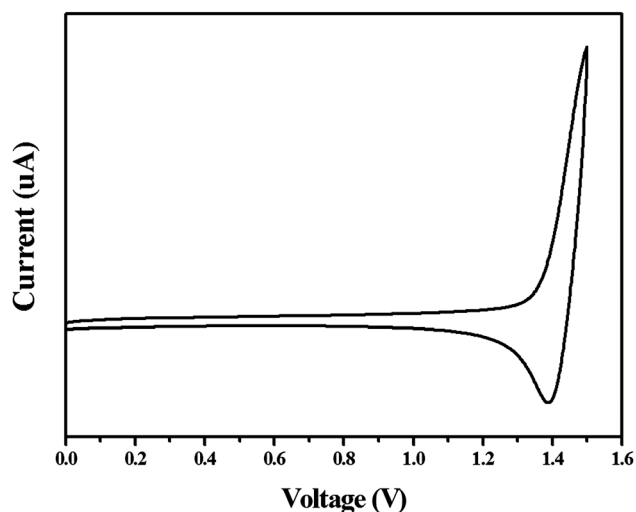
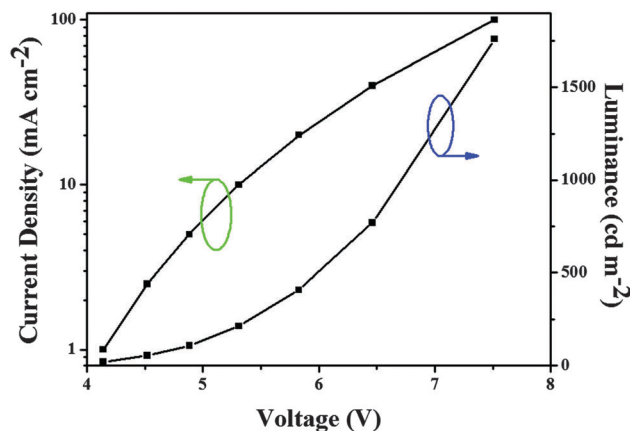
Fig. 4 Cyclic voltammogram of DPSBAF in CH_2Cl_2 .

Fig. 5 Current density–voltage–luminance characteristics of the DPSBAF device.

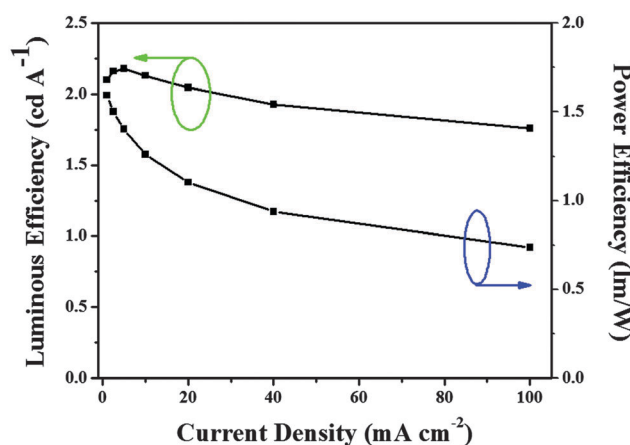


Fig. 6 Luminescent efficiency curve and power efficiency curve versus current density for the DPSBAF device.

The current density–voltage–luminance characteristics of the device are shown in Fig. 5. As shown in Fig. 6, the maximum luminance efficiency for DPSBAF was found to be 2.18 cd A^{-1} , and the power efficiency (PE) was found to be 1.59 lm W^{-1} at 1 mA cm^{-2} . The maximum external quantum efficiency of the DPSBAF non-doped OLED was 2.87% (see Fig. 7). The maximum emission λ_{max} of DPSBAF was located at 448 nm, and the FWHM value was 84 nm. Compared with PL, it is common that there is a 23 nm red-shift for the emission peak in the EL spectrum.^{39,40} The red-shift can be ascribed to face-to-face π - π stacking in the vacuum-deposited film, unlike the randomly arranged molecules in the spin-coated film.^{23,41} When the current density was 20 mA cm^{-2} , the CIE coordinates (x, y) of the DPSBAF device were found to be (0.15, 0.09), which is close to the blue standard (0.14, 0.08) of the NTSC. The EL properties of the DPSBAF device are summarized in Table 2.

4. Conclusions

In summary, a spiro[benzoanthracene–fluorene] derivative, namely DPSBAF, with a T_g of $210 \text{ }^\circ\text{C}$ was designed and synthesized for use as a deep-blue emitter in a non-doped OLED. The

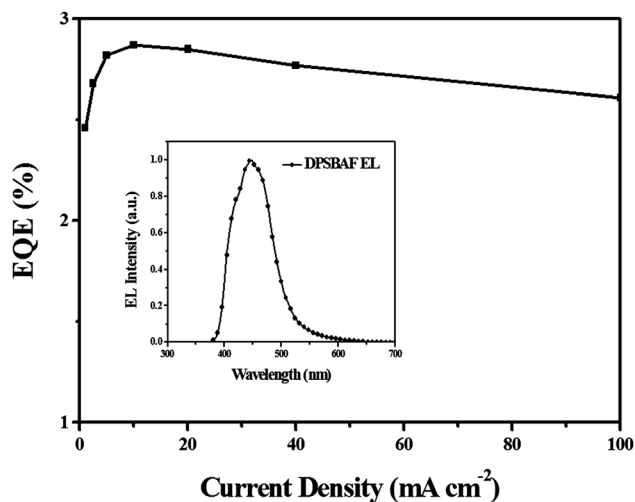


Fig. 7 The external quantum efficiency and EL spectra of the DPSBAF OLED.

device based on DPSBAF exhibited a maximum LE of 2.18 cd A⁻¹ with a maximum EQE of 2.87%. A saturated deep-blue emission with CIE coordinates of (0.15, 0.09) was achieved by using DPSBAF as the emitter. DPSBAF showed a high thermal stability and potential for application in non-doped saturated deep-blue OLEDs.

Acknowledgements

This work was given financial support from the National Natural Science Foundation of China (51273209, 21102156), Ningbo International Cooperation Foundation (2012B10022, 2012D10009, 2013D10013) and External Cooperation Program of the Chinese Academy of Sciences (No. GJHZ1219).

Notes and references

- W. J. Li, D. D. Liu, F. Z. Shen, D. G. Ma, Z. M. Wang, T. Feng, Y. X. Xu, B. Yang and Y. G. Ma, *Adv. Funct. Mater.*, 2012, **22**, 2797.
- L. Yao, S. T. Zhang, R. Wang, W. J. Li, F. Z. Shen, B. Yang and Y. G. Ma, *Angew. Chem., Int. Ed.*, 2014, **126**, 2151.
- L. Li, J. J. Liang, S.-Y. Chou, X. D. Zhu, X. F. Niu, Z. B. Yu and Q. B. Pei, *Sci. Rep.*, 2014, **4**, 1.
- Y. Yuan, D. Li, X. Q. Zhang, X. J. Zhao, Y. Liu, J. Y. Zhang and Y. Wang, *New J. Chem.*, 2011, **35**, 1534.
- K. E. Linton, A. L. Fisher, C. Pearson, M. A. Fox, L.-O. Pålsson, M. R. Bryce and M. C. Petty, *J. Mater. Chem.*, 2012, **22**, 11816.
- H. Fukagawa, T. Shimizu, N. Ohbe, S. Tokito, K. Tokumaru and H. Fujikake, *Org. Electron.*, 2012, **13**, 1197.
- X. H. Ouyang, X. Y. Zhang and Z. Y. Ge, *Dyes Pigm.*, 2014, **103**, 39.
- I. Cho, S. H. Kim, J. H. Kim, S. Parka and S. Y. Park, *J. Mater. Chem.*, 2012, **22**, 123.
- X. Xing, L. X. Xiao, L. L. Zheng, S. Y. Hu, Z. J. Chen, B. Qu and Q. H. Gong, *J. Mater. Chem.*, 2012, **22**, 15136.
- W. Wan, H. L. Du, J. Wang, Y. P. Le, H. Z. Jiang, H. Chen, S. Z. Zhu and J. Hao, *Dyes Pigm.*, 2013, **96**, 642.
- A. L. Fisher, K. E. Linton, K. T. Kamtekar, C. Pearson, M. R. Bryce and M. C. Petty, *Chem. Mater.*, 2011, **23**, 1640.
- L. Yao, S. F. Xue, Q. Wang, W. Y. Dong, W. Yang, H. B. Wu, M. Zhang, B. Yang and Y. G. Ma, *Chem. – Eur. J.*, 2012, **18**, 2707.
- L. Yao, S. H. Sun, S. F. Xue, S. T. Zhang, X. Y. Wu, H. H. Zhang, Y. Y. Pan, C. Gu, F. H. Li and Y. G. Ma, *J. Phys. Chem. C*, 2013, **117**, 14189.
- Y.-C. Chang, S.-C. Yeh, Y.-H. Chen, C.-T. Chen, R.-H. Lee and R.-J. Jeng, *Dyes Pigm.*, 2013, **99**, 577.
- B. A. Kamino, Y.-L. Chang, Z.-H. Lu and T. P. Bender, *Org. Electron.*, 2012, **13**, 1479.
- Y. Zhang, S.-L. Lai, Q.-X. Tong, M.-F. Lo, T.-W. Ng, M.-Y. Chan, Z.-C. Wen, J. He, K.-S. Jeff, X.-L. Tang, W.-M. Liu, C.-C. Ko, P.-F. Wang and C.-S. Lee, *Chem. Mater.*, 2012, **24**, 61.
- X. Xing, L. P. Zhang, R. Liu, S. Y. Li, B. Qu, Z. J. Chen, W. Sun, L. X. Xiao and Q. H. Gong, *ACS Appl. Mater. Interfaces*, 2012, **4**, 2877.
- T. P. I. Saragi, T. Spehr, A. Siebert, T. Fuhrmann-Lieker and J. Salbeck, *Chem. Rev.*, 2007, **107**, 1057.
- D. Thirion, M. Romain, J. Rault-Berthelot and C. Poriol, *J. Mater. Chem.*, 2012, **22**, 7149.
- J.-Y. Kim, C.-W. Lee, J. G. Jang and M.-S. Gong, *Dyes Pigm.*, 2012, **94**, 304.
- M.-J. Kim, C.-W. Lee and M.-S. Gong, *Dyes Pigm.*, 2014, **105**, 202.
- H. J. Liang, X. X. Wang, X. Y. Zhang, Z. Y. Ge, X. H. Ouyang and S. D. Wang, *Dyes Pigm.*, 2014, **108**, 57.
- H. Park, J. Lee, I. Kang, H. Y. Chu, J.-I. Lee, S.-K. Kwon and Y.-H. Kim, *J. Mater. Chem.*, 2012, **22**, 2695.
- Y.-H. Chen, S.-L. Lin, Y.-C. Chang, Y.-C. Chen, J.-T. Lin, R.-H. Lee, W.-J. Kuo and R.-J. Jeng, *Org. Electron.*, 2012, **13**, 43.
- C.-J. Zheng, W.-M. Zhao, Z.-Q. Wang, D. Huang, J. Ye, X.-M. Ou, X.-H. Zhang, C.-S. Lee and S.-T. Lee, *J. Mater. Chem.*, 2010, **20**, 1560.
- Q. Wang, I. W. H. Oswald, M. R. Perez, H. P. Jia, B. E. Gnade and M. A. Omary, *Adv. Funct. Mater.*, 2013, **23**, 5420.
- Q. Wang, I. W. H. Oswald, M. R. Perez, H. P. Jia, A. A. Shahub, Q. Q. Qiao, B. E. Gnade and M. A. Omary, *Adv. Funct. Mater.*, DOI: 10.1002/adfm.201400597.
- M. Weimar, G. Dürner, J. W. Bats and M. W. Göbel, *J. Org. Chem.*, 2010, **75**, 2718.
- M. Lejeune, P. Grosshans, T. Berclaz, H. Sidorenkova, C. Besnard, P. Pattison and M. Geoffroy, *New J. Chem.*, 2011, **35**, 2510.
- X. Q. Zhang, Z. G. Chi, B. J. Xu, H. Y. Li, Z. Y. Yang, X. F. Li, S. W. Liu, Y. Zhang and J. R. Xu, *Dyes Pigm.*, 2011, **89**, 56.
- J. H. Huang, J.-H. Su, X. Li, M.-K. Lam, K.-M. Fung, H.-H. Fan, K.-W. Cheah, C. H. Chen and H. Tian, *J. Mater. Chem.*, 2011, **21**, 2957.

- 32 S. Tang, W. J. Li, F. Z. Shen, D. D. Liu, B. Yang and Y. G. Ma, *J. Mater. Chem.*, 2012, **22**, 4401.
- 33 H. Wang, H. S. Lim, S. Kim, J. Lim, C. Lee and D. W. Kim, *Synth. Met.*, 2009, **159**, 2564.
- 34 S. Kim, T. K. An, J. Chen, I. Kang, S. H. Kang, D. S. Chung, C. E. Park, Y.-H. Kim and S.-K. Kwon, *Adv. Funct. Mater.*, 2011, **21**, 1616.
- 35 T. K. An, S.-H. Hahn, S. Nam, H. Cha, Y. Rho, D. S. Chung, M. Ree, M. S. Kang, S.-K. Kwon, Y.-H. Kim and C. E. Park, *Dyes Pigm.*, 2013, **96**, 756.
- 36 H. Q. Zhang, X. J. Wan, X. S. Xue, Y. Q. Li, A. Yu and Y. S. Chen, *Eur. J. Org. Chem.*, 2010, 1681.
- 37 H. Sasabe, E. Gonmori, T. Chiba, Y.-J. Li, D. Tanaka, S.-J. Su, T. Takeda, Y.-J. Pu, K. Nakayama and J. Kido, *Chem. Mater.*, 2008, **20**, 5951.
- 38 J.-Y. Hu, Y.-J. Pu, Y. Yamashita, F. Satoh, S. Kawata, H. Katagiri, H. Sasabe and J. Kido, *J. Mater. Chem. C*, 2013, **1**, 3871.
- 39 Z.-Q. Liang, Z.-Z. Chu, D.-C. Zou, X.-M. Wang and X.-T. Tao, *Org. Electron.*, 2012, **13**, 2898.
- 40 X. J. Feng, S. F. Chen, Y. Ni, M. S. Wong, M. M. K. Lam, K. W. Cheah and G. Q. Lai, *Org. Electron.*, 2014, **15**, 57.
- 41 X. Xing, L. W. Zhong, L. P. Zhang, Z. J. Chen, B. Qu, E. Q. Chen, L. X. Xiao and Q. H. Gong, *J. Phys. Chem. C*, 2013, **117**, 25405.